JOURNAL OF CATALYSIS 38, 312–325 (1975)

Characterization of Acid–Base Catalysts by Calorimetric Titration

I. Correlation with Alcohol Dehydration Activity

K. R. BAKSHI[1] AND G. R. GAVALAS[2]

Division of Chemistry and Chemical Engineering, California Institute of Technology, Pasadena, California 91125

Received December 12, 1974

Several commercial aluminas, silica–aluminas and clays are characterized by calorimetric titration with *n*-butylamine and trichloroacetic acid. The heat of adsorption distributions obtained by titration are found to be sufficient measures of surface acidity and basicity in correlating catalyst activity towards alcohol dehydration. A correlation is obtained by dividing the distributions into groups of suitable acidic and basic site pairs, and assigning to each group a specific reaction rate by least-squares fitting with the observed rates of dehydration. The correlation describes well both olefin and ether formation and provides support for a reaction mechanism proposed in the literature.

NOMENCLATURE

A_i	Acidity in *i*th group defined in Table 5
B_i	Basicity in *i*th group defined in Table 6
f_i	Specific rate for *i*th group
r	Rate of product formation, mol product/hr-g catalyst
r_{ob}	Experimentally observed rate of product formation
r_{pr}	Predicted rate of product formation
r_j	Rate of product formation for *j*th catalyst
s_{ij}	Effective site density in *i*th group for *j*th catalyst
W	Amount of titer adsorbed, mmol/g catalyst
$-\Delta H$	Heat of adsorption, kcal/mol
σ	Selectivity defined in Table 2
σ_{ob}	Experimentally observed selectivity
σ_{pr}	Predicted selectivity

[1] Now with Chevron Research Co., Richmond, CA 94802.

[2] To whom correspondence should be directed.

INTRODUCTION

Catalyst development and utilization requires information about the dependence of the catalyst activity and selectivity on the state of the catalyst as well as the modification of the catalyst state due to pretreatment and deactivation processes. Such an interrelation between pretreatment or deactivation, catalyst state, and reaction kinetics presupposes, above all, a suitable and reproducible method of catalyst characterization. Site density or surface area has served as one important parameter characterizing various catalysts but is clearly insufficient for catalysts possessing sites of various strengths. A proper characterization includes specification of a strength parameter along with corresponding capacity parameter thus resulting in a site strength distribution, characteristic of the catalyst state.

Acidic catalysts such as alumina, silica–alumina and zeolites display a particularly wide variation in site strength and have been studied by a number of different methods. A review of the methods for the

determination of the surface acidity distribution has been given by Tanabe (*16*).

Originally reported by Walling (*19*) and Benesi (*3*), a colorimetric titration of acidic catalysts with an *n*-butylamine solution using a variety of Hammett indicators has been extensively employed by many workers. Hirschler (*8*) improved upon these titrations by using H_R indicators and showed that Hammett indicators fail to resolve acidities of catalysts with different activities. Both these titrations characterize the catalyst surface in terms of an acidity distribution divided into distinct groups of acidic strengths equivalent to the acidity constants of the various indicators employed. The titer value within each group serves as a capacity parameter to represent the site density possessing the corresponding group strength.

Adsorption of a gaseous base such as ammonia followed by evacuation of the catalyst at various temperatures [Webb (*20*)] or a differential thermal analysis [Bremer and Steinberg (*4*)] has also been employed to characterize acidic catalysts. The evacuation temperature and the amount of base retention serve as the strength and capacity parameter, respectively. Amenomiya and Cvetanović (*1*) have developed a temperature programmed desorption technique to obtain site strength in terms of desorption temperature. Topchieva *et al.* (*18*) and Tanabe and Yamaguchi (*15*) developed calorimetric titrations to obtain the total acidity of various catalysts by measuring the heat of adsorption of a base. The heat of adsorption and the titer values serve as the strength and capacity parameters, respectively.

Although all these methods have been employed to characterize acidic catalysts, some of them show distinct limitations when used in certain specific cases. The thermal adsorption–desorption techniques are restricted to thermally stable gaseous bases and hence are useful in characterizing the catalysts possessing relatively weak sites only. Since the colorimetric titrations depend upon visual changes of indicator colors, they cannot be easily employed in characterizing colored acidic catalysts. Moreover, the color changes for some of the Hammett indicators are not easily perceptible, thereby introducing uncertainty in results, Drushel and Sommers (*6*).

In conjunction to their acidic sites, the catalysts under discussion possess basic sites [Peri (*11*)], which play an important role in certain reactions such as alcohol dehydration, Pines and Manassen (*13*), Bakshi and Gavalas (*2*). The characterization of the basicity using colorimetric titrations has not been possible [Tanabe and Yamaguchi (*15*)] due to unavailability of suitable indicators. Calorimetric titration on the other hand has been used successfully for estimating the total number of basic sites of a silica–alumina catalyst, Tanabe (*16*).

The most useful aspect of a catalyst characterization method is its ability to distinguish between catalysts of different activities and to correlate the activity with the capacity parameter of the catalyst. Development of such correlations have been extensively attempted for acidic catalysts using one of the methods described earlier. Pines and Haag (*12*) have investigated the activity of aluminas in alcohol dehydration and hydrocarbon isomerization reactions and have related it to number and strength of acidic sites as determined by amine chemisorption and colorimetric indicators. Polymerization of olefins [Tarama *et al.* (*17*)], xylene isomerization and cracking of cumene [Covini *et al.* (*5*)] and catalytic cracking [Mone and Moscou (*10*)] have all been investigated on silica–alumina and zeolites to show good correlation between the catalyst activity and the total acidity measured by amine titrations. Such correlations between catalyst activity and acidity have been reviewed by Tanabe

(*16*). Most of the correlations employ either total acidity or acidity above certain indicator levels to represent the total number of active sites. The contribution of the various sites is assumed to be the same, independent of site strength.

Since a nonuniform catalyst owes its activity to sites having distinctly different strengths, the contribution from various sites is not expected to be identical. Yoneda (*22*) has attempted to correlate activity of nonuniform catalysts for olefin oligomerization by employing amine titrations to characterize acidity distributions. Investigating a sufficient number of comparable catalysts, he has obtained the relative activity of sites having different acidic strength. It must be noted that most of the aforementioned correlations were developed for single reactions and have not attempted to describe catalyst selectivity in the case of competitive reactions.

The present work is concerned with the characterization of acid–base catalysts in terms of their acidity and basicity distributions and attempts to correlate their acid–base characteristics with their activity for the dehydration of methanol and ethanol. The dehydration of alcohols by alumina and silica–alumina has been studied extensively by Winfield (*21*), Pines and Manassen (*13*) and Figueras *et al.* (*7*). The reactions have been shown to require basic as well as acidic sites (*7*), therefore the present work has emphasized the distribution of both functions. Among various methods of catalyst characterization, calorimetric titration providing the heat of adsorption as a function of coverage has been found to be the most convenient as a measure of the acidity and basicity distributions. Since the dehydration of ethanol provides ethylene and ether, the correlation developed here includes the catalyst selectivity as well as its activity.

EXPERIMENTAL METHODS

1. Reagents. Reagent grade methanol, ethanol and *n*-butylamine were used without further purification. Reagent grade benzene was dried by percolation over a molecular sieve bed before use. Anhydrous ammonia, supplied by Matheson Gas Products, was used without further purification.

2. Catalysts. Commercial catalysts used for this investigation are shown in Table 1. The pelleted catalysts were finely crushed and fractionated under dry nitrogen to prevent contamination. All catalyst samples were pretreated at 300°C under dry nitrogen for 5 hr and stored under dry conditions before use.

Two of the commercial catalysts, KSFO and AHC, were impregnated with MgO using aqueous solution of magnesium acetate followed by calcining at 500°C for 4 hr.

3. Activity measurements. Evaluation of catalyst activity for alcohol dehydration was carried out in a differential microreactor suspended in a well-mixed air bath. The reactor temperature was maintained within ±0.2°C of the reported values by a proportional temperature controller. Alcohol, fed by a multispeed infusion pump, was vaporized and mixed

TABLE 1
COMERCIAL CATALYSTS FOR ALCOHOL DEHYDRATION

Catalyst code	Supplier	Chemical composition
KSF	Chemetron Corp.	Acid treated montmorillonite clay
KSFO	Chemetron Corp.	Acid treated montmorillonite clay
F49	Filtrol Corp.	74% SiO_2 17.5% Al_2O_3 4.5% MgO
AHC	American Cyanamid Co.	75% SiO_2 25% Al_2O_3
ALC	American Cyanamid Co.	87% SiO_2 13% Al_2O_3
T-126	Chemetron Corp.	Activated γ-alumina
F1	Aluminum Co. of America	γ-Alumina

with dry nitrogen to attain the desired feed concentration. The reaction products were analyzed by a flame ionization detector after separation on a 10% Carbowax 20 m column. The details of the experimental setup are described elsewhere (*2*).

4. Ammonia adsorption capacity. Thermogravimetric analysis was employed to quantitatively obtain the ammonia adsorption capacity of various catalysts. A 950 DuPont TGA system was used to determine the decrease in weight of a catalyst sample upon thermal desorption at various temperatures. The TGA assembly was flushed at room temperature with flowing helium for 2 hr and about 40–50 mg of powdered catalyst sample were placed in the sample pan of the TGA. The catalyst sample was heated to 500°C under flowing dry helium, was maintained at that temperature for 1 hr, and was subsequently cooled to room temperature under dry helium. The sample was then saturated with ammonia by passing anhydrous ammonia for 2 hr until no further increase in weight could be recorded. After discontinuing the ammonia flow, the TGA chamber was flushed with helium and the temperature of the sample was raised and maintained at 150°C under dry helium until no further weight decrease due to ammonia desorption could be detected. This procedure was repeated at 50°C temperature increments up to 500°C and the sample weight was continuously recorded. This procedure enabled an estimation of the ammonia adsorption capacity of various catalysts at different temperatures.

5. Rate recovery experiments. The partial recovery of activity attendant upon thermal desorption of a weak poison such as ammonia was used as another characterization of various catalysts. The catalyst sample was pretreated to 500°C, as indicated earlier, and was subsequently cooled to 100°C. Ammonia diluted with dry nitrogen was passed over the catalyst for 4 hr to completely saturate the sample at that temperature. The flow of ammonia was then discontinued and the catalyst was heated to a higher temperature under dry nitrogen flow. The thermal desorption was carried out for 2 hr after which the activity of the catalyst for alcohol dehydration reaction was measured in the flow microreactor. This procedure was repeated at different desorption temperatures for all catalysts.

6. Calorimetric titrations. In principle, calorimetric titrations involve measurements of heat of adsorption of a liquid reactant as a function of the amount adsorbed. In the present study the calorimetric assembly consisted of a Dewar flask equipped with a Beckmann thermometer, a magnetic stirrer and a microburette, and was insulated with a thick cork. About 3–5 g of powdered, pretreated catalyst were placed in 100 ml dry benzene in the Dewar flask and stirred. The contents of the calorimeter were allowed to equilibrate with the surroundings for about 1 hr before the titrations. The temperature rise due to stirring was read at definite time intervals. The titrations were carried out by stepwise addition of aliquots (0.3–0.5 ml) of a standardized reactant from a microburette. The bath temperature was read every 30 s for about 10–15 min after each addition. The total rise in temperature was corrected for the slight contribution from stirring to give the rise due to the heat of adsorption. The latter temperature rise was observed to level off after about 2–3 min after each addition.

The above procedure was repeated with subsequent increments of reactant additions until no temperature rise due to heat of adsorption could be observed. The standardized reactant solutions were 0.909 *M* *n*-butylamine in dry benzene for acidity measurements and 0.44 *M* trichloroacetic acid in dry benzene for basicity measurements. The heat capacity of the calorimeter and its contents was evaluated by measuring the temperature rise in 10 min due to passage of a dc electric current through a Nichrome wire heater immersed in the

calorimeter. The energy input in this time interval was estimated from voltage drop measurements across the Nichrome heater and a 1.69 ohm standard resistor in series with the heater.

A theoretical estimation of the time required for liquid phase diffusion in porous catalysts was carried out by a procedure described in Ref. (*14*) using an effective tortusoity factor of 6 and porosity of 0.4 for the powdered catalysts. The estimated value of the diffusion coefficient was 2×10^{-6} cm^2/s with a corresponding characteristic diffusion time of 1–2 min for 100 μm particles. It follows that the observation time of 10–15 min for each incremental titer addition is sufficient for completion of chemisorption provided the kinetics of chemisorption is not rate limiting.

RESULTS

1. Activity measurements. The activity of various commercial catalysts for dehydration of methanol and ethanol was measured under identical conditions of feed concentration and temperature. The only products observed were dimethyl ether during methanol dehydration and diethyl ether and ethylene during ethanol dehydration. The rates of formation of various products listed in Table 2 show wide variations of activity and selectivity among the nine catalysts tested.

2. Ammonia adsorption capacity. Since the dehydration activity of the catalysts tested is known to be impaired by chemisorption of ammonia and organic bases, a correlation was attempted between the ammonia adsorption capacity and the activity of the catalysts. The results of the thermogravimetric analysis of F49, AHC and F1 catalysts are shown in Table 3 in terms of ammonia retained at various temperatures. The adsorption capacity of a catalyst sample at a given desorption temperature is evaluated from the difference in weight of the sample at that temperature and the weight of the dry catalyst at 500°C. The results in Table 3 indicate that ammonia adsorption capacity at temperatures above 250°C is in the order F49 > AHC > F1. As shown in Table 2, the activity for both ether and olefin formation follows the same order. The result is not surprising since the ammonia retained at higher desorption temperatures is attached to the stronger sites which are expected to make the major contribution to the dehydration reactions. Although reactivity and ammonia adsorption capacity maintain the same order among the catalysts, a quantitative correlation between

TABLE 2
DEHYDRATION ACTIVITY OF VARIOUS CATALYSTS

Catalyst	Rate of product formation[a] Dimethyl ether ($r \times 10^3$)	Ethylene ($r \times 10^4$)	Diethyl ether ($r \times 10^3$)	Percentage selectivity[b] σ
KSFO	30.98	105.3	29.9	14.97
KSFO + M[c]	25.1	62.4	24.0	11.50
KSF	3.05	33.8	2.98	36.20
F49	12.47	26.9	14.20	8.65
LAC	3.25	5.66	2.39	10.60
AHC	2.00	1.10	1.30	4.06
AHC + M[c]	2.69	1.00	1.54	3.15
T126	4.58	0.105	2.27	0.23
Fl	0.197	0.027	0.129	1.04

[a] Experimental conditions: reaction temp, 200°C; feed methanol concn, 6.77×10^{-3} mol/liter; feed ethanol concn, 6.64×10^{-3} mol/liter.

[b] Selectivity σ is defined by

$$\sigma = \frac{\text{amount of ethanol converted to ethylene}}{\text{total ethanol conversion}} \times 100.$$

[c] Catalysts + M denote impregnated catalysts.

TABLE 3
AMMONIA ADSORPTION CAPACITY OF VARIOUS CATALYSTS

Desorption temp (°C)	Ammonia retained (mmol/g catalyst) F49	AHC	Fl
400	0.2522	0.1582	0.1188
350	0.5156	0.3640	0.1422
300	0.7408	0.5974	0.2633
250	0.9343	0.8655	0.4197
200	1.1471	1.1742	0.6102
150	1.4700	1.5452	0.8572

the two properties does not appear feasible in view of the fact that reactivity varies much more rapidly than ammonia adsorption capacity. For example, F49 shows a 1000-fold activity for olefin formation as compared to F1, while the corresponding ammonia adsorption capacity ratio is only two even for the strongest sites measured at 450°C. A further desorption at temperatures above 500°C may perhaps be required to provide a significant distinction between the two catalysts. Furthermore, although the catalytic activities for both ether and olefin formation follow the same qualitative order as that of acidity evaluated in terms of ammonia adsorption capacity, the relative variations in the selectivity shown in Table 2 indicate that the catalyst characterization follows different correlative patterns for the two dehydration reactions.

3. Rate recovery experiments. The relative recovery of catalyst activity attendant upon desorption of ammonia at various desorption temperatures is reported in Table 4 for F49, AHC and F1 catalysts. The activity recovery at all desorption temperatures follows the order F1 > AHC > F49 for both ether and olefin formation, thus indicating that weaker sites are responsible for the activity of F1 whereas much stronger sites are responsible for the activity of F49. These results show the same trend with the relative activities of these catalysts as shown in Table 2 as well as with the ammonia adsorption capacity as shown in Table 3. The relative recovery pattern for olefin formation in comparison with ether formation for all catalysts tested indicate that the effect of ammonia adsorption is larger on ethylene than on ether formation at all desorption temperatures. From the difference in relative recovery rates between two successive desorption temperatures, it is apparent that the stronger acidic sites contribute more to the activity than the weaker sites. Any attempt at a characterization of these catalysts would thus involve the intrinsic heterogeneity of the catalyst surface in terms of its acidity distribution.

TABLE 4
ACTIVITY RECOVERY FOR VARIOUS CATALYSTS

Desorption temp (°C)	Percentage activity recovery[a]					
	F49		AHC		F1	
	Ethylene	Ether	Ethylene	Ether	Ethylene	Ether
200	2.08	4.35	28.97	49.00	71.30	89.92
250	2.64	4.50	32.35	66.57	—[b]	—[b]
300	5.62	11.60	40.00	74.79	87.04	97.67
350	14.50	23.40	46.20	77.38	97.80	99.00
400	26.80	33.80	59.70	87.25	—	—
465	47.50	70.00	97.80	98.87	—	—

[a] Experimental conditions: alcohol feed concentration, 6.64×10^{-3} mol/liter; reaction temp, 200°C.
[b] Data not available.

4. Calorimetric titrations. Calorimetric titration of solid catalysts against standard reagents involves evaluation of heat of adsorption from a knowledge of heat capacity of the calorimetric system and the temperature rise upon addition of a differential amount of the reagent to the calorimeter. The heat release thus calculated represents an average heat of chemisorption for the amount of reagent added. The titration results are thus obtained as average differential heats of chemisorption for successive equal additions of the reagent. The results for various catalysts titrated are as follows:

a. ACIDITY DISTRIBUTION. The calorimetric titrations for acidity measurements are reported in terms of heat of adsorption of *n*-butylamine solution at room temperature. A representative set of differential heat of adsorption curves is shown in Fig. 1 for some of the catalysts. Invoking an assumption that chemisorption of *n*-butylamine on a stronger acidic site results in a higher heat of adsorption, the acidic strength of these catalysts can be arranged in the order KSFO > F49 > AHC > F1. Since the same order is exhibited in their relative activities (Table 2), the acidity

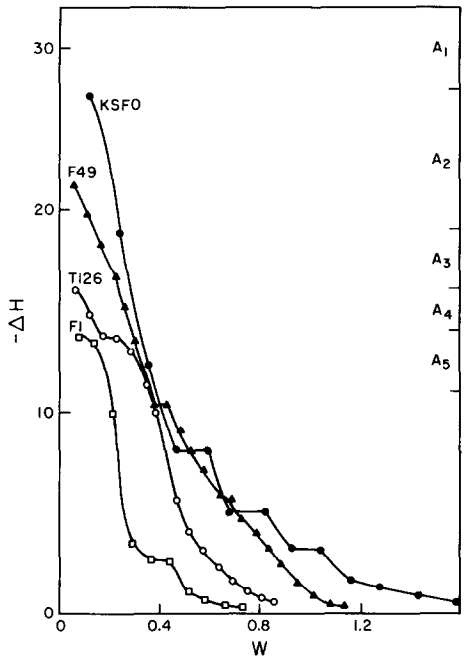

FIG. 1. Heat of adsorption versus *n*-butylamine coverage.

measurements obtained through calorimetric titrations appear to provide a good method for catalyst characterization.

In order to obtain a quantitative correlation between the acidity distribution and the relative activities of the various catalysts, the differential heat curves are divided into groups each of which spans a range of heats of adsorption as indicated in Fig. 1. The limits of each group are selected by an inspection of the relative activities of various catalysts. Table 5 shows the acidity distributions in terms of groups A_1–A_5 of Fig. 1. Assuming that all acidic sites contribute to the catalytic activity and that the relative contributions depend upon the strength of the acidic sites, there appears to be a general qualitative agreement between the relative activities (Table 2) and the acidity distributions shown in Table 5.

The acidity distributions follow the same order as the ammonia adsorption capacity of F49, AHC and F1 catalysts. The results obtained in the rate recovery experiments are also in good qualitative agreement with the acidity distributions of Table 5 in that the weaker sites of F1 show higher rate recovery upon thermal desorption of ammonia as compared to the AHC and F49 catalysts.

TABLE 5
ACIDITY DISTRIBUTIONS OF VARIOUS CATALYSTS

Catalyst	Acidity[a] (mmol/g catalyst)				
	A_1	A_2	A_3	A_4	A_5
KSFO	0.0	0.24	0.05	0.04	0.06
KSFO + M	0.0	0.21	0.06	0.05	0.11
KSF	0.033	0.037	0.015	0.012	0.015
F49	0.0	0.136	0.104	0.06	0.09
ALC	0.0	0.02	0.22	0.08	0.13
AHC	0.0	0.0	0.24	0.08	0.15
AHC + M	0.0	0.0	0.22	0.05	0.07
T126	0.0	0.0	0.0	0.168	0.184
Fl	0.0	0.0	0.0	0.0	0.20
KSFO + 0.12 KOH[b]	0.0	0.115	0.055	0.05	0.08

[a] Acidity groups are defined by heat of adsorption included between limits as follows: A_1: $26 < -\Delta H$; A_2: $19 < -\Delta H < 26$; A_3: $16 < -\Delta H < 19$; A_4: $14 < -\Delta H < 16$; A_5: $11 < -\Delta H < 14$.

[b] KSFO titrated with 0.12 mmol/g catalyst KOH in aqueous solution before pretreatment.

Before proceeding further we may note certain properties of the acidity distributions that are important in the group analysis given below. For all the catalysts titrated, the differential heat curves are concave in nature, indicating a decrease in differential heat of adsorption upon subsequent additions of *n*-butylamine. This effect may result from either inherent heterogeneity of the catalyst surface or from the effect of previously adsorbed *n*-butylamine which may render the neighboring acidic sites weaker by induction. Since the surface induction effect would be expected to be different for other bases, a partial titration of the catalyst to a known extent by a stronger base such as KOH, followed by calorimetric titration with *n*-butylamine, is generally expected to result in a complementary acidity distribution only if the inductive effect is insignificant during these titrations. The results in Table 5 indicate that upon partial titration of KSFO with 0.12 mmol/g of KOH, an equivalent number of strong acidic sites of A_2 are

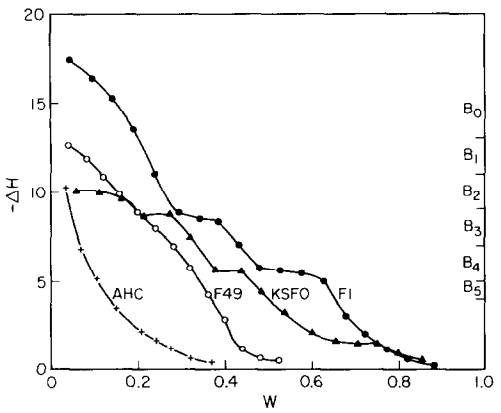

FIG. 2. Heat of adsorption versus trichloroacetic acid coverage.

TABLE 6
BASICITY DISTRIBUTION OF VARIOUS CATALYSTS

Catalyst	Basicity[a] (mmol/g catalyst)				
	B_1	B_2	B_3	B_4	B_5
KSFO	0.0	0.22	0.15	0.13	0.045
KSFO + M	0.12	0.03	0.05	0.09	0.035
KSF	0.0	0.05	0.03	0.02	0.050
F49	0.11	0.09	0.09	0.06	0.025
ALC	0.0	0.06	0.21	0.06	0.03
AHC	0.0	0.044	0.014	0.041	0.03
AHC + M	0.035	0.08	0.014	0.03	0.04
T126	0.066	0.064	0.06	0.06	0.04
F1	0.04	0.045	0.144	0.19	0.03

[a] Basicity groups are defined by heat of adsorption included between limits as follows: B_1: $11 < -\Delta H < 13$; B_2: $9 < -\Delta H < 11$; B_3: $7 < -\Delta H < 9$; B_4: $5 < -\Delta H < 7$; B_5: $4 < -\Delta H < 5$.

destroyed as measured by *n*-butylamine titrations. The complementary nature of these titrations suggest that the variations in differential heat curve with coverage results from the inherent surface heterogeneity and not from the surface induction effect of previously absorbed *n*-butylamine. This important issue certainly requires further investigation.

b. BASICITY DISTRIBUTIONS. The basicity measurements of various catalysts obtained by calorimetric titrations are reported in terms of differential heats of adsorption of trichloroacetic acid. A representative set of differential heat curves is shown in Fig. 2 for some of the catalysts. The variation in the differential heat of adsorption with successive additions of the reactant indicates the heterogeneity of the catalyst surface. As in the case of the acidity distributions, the differential heat curves for basicity have been divided into groups of basicities as indicated in Fig. 2, and the basicity distributions thus obtained are shown in Table 6. The presence of MgO in impregnated catalysts and in F49 is evidently related to the strong basicities of these catalysts. In agreement with observations reported recently by Figueras *et al.* (*7*), the γ-alumina T126 and F1 possess stronger basicity than silica–alumina.

The results of acidity and basicity titrations on AHC using different amounts of stepwise additions are shown in Fig. 3. The differential heat curves for acidity and basicity depicted in Fig. 3 indicate the reproducibility of the titrations.

5. Catalyst characterization and group analysis. The qualitative agreement among the results obtained in ammonia adsorption experiments, rate recovery experiments, relative activities for dehydration reactions and the acid–base distributions obtained by calorimetry suggest that these characteristics could be utilized to develop a quantitative correlation for the activities

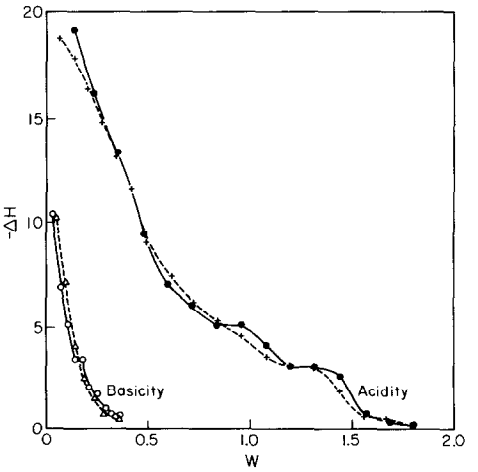

FIG. 3. Effect of titer increment on the heat of adsorption curves of AHC. Titer increment (mmol/g catalyst): (●) 0.120; (+) 0.0705; (△) 0.0458; (○) 0.0358.

and selectivities of the catalysts tested. The surface heterogeneity suggests that the acid–base sites of each catalyst may be subdivided into groups of different strengths so that the catalytic activity observed for a given chemical reaction is a sum of contributions from all such active groups.

All the active sites within a group are assumed to contribute equally to the overall catalyst activity independently of the catalyst considered. Thus the contribution by a group i to the activity of the jth catalyst is given by $(f_i s_{ij})$ where f_i, the specific rate, depends on the strength of the group i, reactant concentration and temperature but not on the catalyst state. Under these assumptions, the overall reaction rate r_j on jth catalyst of unit weight can be expressed as:

$$r_j = \sum_{i=1}^{N} f_i s_{ij}, \qquad (1)$$

where N is the number of effective groups. The site density s_{ij} for each catalyst can be estimated from the strength distribution obtained by experimental methods such as calorimetric titrations. The reaction rate data for M different catalysts under identical concentration and temperature conditions, along with a detailed knowledge of their strength distributions, enable an estimate of the specific rates f_i by the method of least squares provided M, the number of catalysts tested, is larger than N, the number of groups used to correlate the catalytic activities.

6. Group analysis for ethylene formation. The reaction mechanism discussed earlier [Figueras *et al.* (*7*)] for ethylene formation requires a dissociative chemisorption of alcohol on an acid–base site pair, where strong acidity is more effective. Since the presence of a basic site is necessary for adsorption and subsequent reaction, only those acidic sites which have adequate basicity in their neighborhood are effective. A determination of the effective site density s_{ij} to be used for group analysis thus requires consideration of acid–base pairs of varying acidic and basic strengths. The acidity and basicity groups used for this investigation are shown in Tables 5 and 6 for various catalysts. Different models involving association of an acidic site with various basic groups alone or in combination are attempted to determine the effective s_{ij}. A set of specific rates f_i is determined by a least-square fit for each model and the fit for different models are compared in terms of their residuals as shown in Table 7. The results in Table 7 imply that a model requiring an interaction between an acidic site with weak basic sites in the groups $(B_4 + B_5)$ gives the best least square fit. Table 8 presents the specific rates and the comparison between observed rates and rates predicted by the group analysis. The agreement between predicted and observed rates is also shown in Fig. 4. The significant variation in the specific rates substantiates the assumption that the contribution to the total activity by acidic sites weaker than the A_5 group is negligible and hence these sites need not be considered in the group analysis. The necessity of a weak basic site for dissociative chemisorption of alcohol and subsequent reaction reported earlier [Figueras *et al.* (*7*)] is

TABLE 7
DETERMINATION OF BEST MODEL FIT FOR ETHYLENE FORMATION

s_{ij}	Sum of weighted residual χ^{2a}
A_i	0.444
$A_i \times (B_5)$	0.0618
$A_i \times (B_4 + B_5)$	0.0045
$A_i \times (B_3 + B_4 + B_5)$	0.630
$A_i \times (B_2 + B_3 + B_4 \times B_5)$	0.395
$A_i \times B_{\text{total}}$	0.292

[a] Sum of weighted χ^2 is evaluated by:

$$\chi^2 = \sum_j \left(\frac{r_{\text{ob},j} - r_{\text{pr},j}}{r_{\text{ob},j}} \right)^2.$$

TABLE 8
GROUP ANALYSIS FIT FOR ETHYLENE FORMATION

Catalyst	Predicted rate by group analysis[a] $r \times 10^4$	Observed rate $r \times 10^4$
KSF	33.8	33.8
KSFO	100.5	105.3
KSFO + M	62.96	62.40
F49	28.1	26.9
AHC	1.11	1.10
AHC + M	0.993	1.00
T126	0.105	0.105
F1	0.027	0.027
ALC	5.576	5.66

[a] Specific rates for best model fit are: $f_1 = 11933.7$; $f_2 = 2379$; $f_3 = 63.01$; $f_4 = 5.608$; $f_5 = 0.614$.

reflected through a better correlative fit of the model using the basicity $(B_4 + B_5)$. Table 9 shows the actual contributions by each group towards ethylene formation. Comparing the relative contribution of the group with the highest acidic strength for a given catalyst to the total observed rate on that catalyst, it is apparent that almost all catalysts tested owe above 90% of their olefin formation activity to their strongest acidic group, with the exception of KSF and ALC catalysts. Even in these two catalysts, the contribution by their strongest

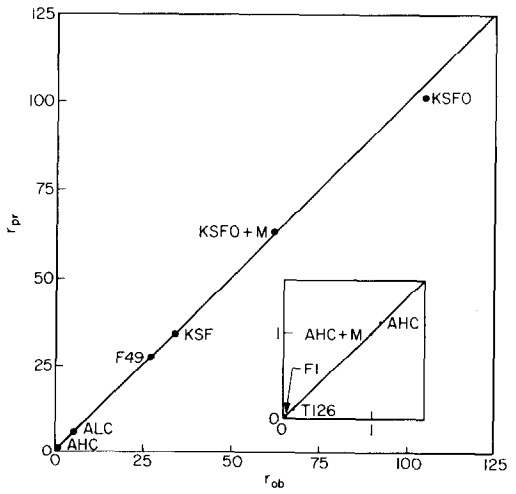

FIG. 4. Group analysis fit for rates of ethylene formation. Experimental conditions: alcohol cencn, 6.64×10^{-3} mol/liter; reaction temp, 200°C.

TABLE 9
DETAILS OF GROUP ANALYSIS FOR ETHYLENE FORMATION

	Group contributions ($r_{ij} \times 10^4$)				
Catalyst j	$f_1 s_{1j}$	$f_2 s_{2j}$	$f_3 s_{3j}$	$f_4 s_{4j}$	$f_5 s_{5j}$
KSF	27.44	6.37	0.07	0.008	0.0008
KSFO	—	99.92	0.56	0.04	0.006
KSFO + M	—	62.45	0.48	0.036	0.007
F49	—	27.50	0.57	0.03	0.005
AHC	—	—	1.073	0.033	0.006
AHC + M	—	—	0.975	0.02	0.003
T126	—	—	—	0.094	0.011
F1	—	—	—	—	0.027
ALC	—	4.282	1.25	0.042	0.006

acidic group is above 75% of the total activity for olefin formation.

7. Group analysis for ether formation. In contrast to the mechanism for olefin formation, the formation of ether has been suggested to involve the interaction between a dissociatively adsorbed alcohol intermediate with a surface alkoxide and involves two acid-base site pairs with strong basicity required for alkoxide formation (*7*). An attempt at applying group analysis to ether formation would thus require a careful consideration of the acid-base distributions while evaluating s_{ij}.

Denoting by X and Y the active sites involved in the dissociative adsorption of alcohol to a carbonium ion and an alkoxide, respectively, we must investigate the acidity and basicity required in each of the two types of sites. The simplification is made that the sites X must be separated to groups X_i due to their wide variation of activities while the Y sites may be considered in a single group. Various models and their fit with the data are listed in Table 10. The models of set A assume that X_i requires acidity alone while Y requires basicity alone, in some optimal range. A comparison of the models in set A shows that $Y = B_1 + B_2$ gives the minimum residual error, thus establishing an optimal span of basicity for alkoxide formation and subsequent reaction to ether.

TABLE 10
BEST MODEL FIT FOR DIETHYL ETHER FORMATION[a]

X_i	Y	Sum of weighted residual χ^2
Set A		
A_i	1.0	0.349
A_i	(B_1)	4.008
A_i	$(B_1 + B_2)$	0.287
A_i	$(B_1 + B_2 + B_3)$	1.209
A_i	$(B_1 + B_2 + B_3 + B_4)$	0.903
A_i	B_{total}	0.742
Set B		
$(A_i) \times (B_4 + B_5)$	(B_1)	4.02
$(A_i) \times (B_4 + B_5)$	$(B_1 + B_2)$	0.409
$(A_i) \times (B_4 + B_5)$	$(B_1 + B_2 + B_3)$	1.371
Set C		
$(A_i) \times (B_4 + B_5)$	$(B_1 + B_2) \times (A_5)$	0.0256
$(A_i) \times (B_4 + B_5)$	$(B_1 + B_2) \times (A_5 + A_4)$	0.0215
$(A_i) \times (B_4 + B_5)$	$(B_1 + B_2) \times (A_5 + A_4 + A_3)$	0.0749

[a] Sum of weighted residual is evaluated by:

$$\chi^2 = \sum_j \left[\frac{r_{\text{ob},j} - r_{\text{pr},j}}{r_{\text{ob},j}} \right]^2.$$

s_{ij} is calculated from (X_i, Y) for jth catalyst.

Since association of strong acidic sites with weak basic sites yields better correlation for ethylene formation which also requires a dissociative adsorption of alcohol, the models in set B of Table 10 explore the effectiveness of the same type of pairs in evaluating X_i. The definition of Y is again based on similar interpretation as for the models of set A. Comparison of the residuals in this set suggests that the best-fit model is the one involving alcohol adsorption on acidic sites associated with weak basic sites in groups $(B_4 + B_5)$, i.e., $X_i = (A_i,\ B_4 + B_5)$, with another alcohol absorbed as an alkoxide on basic groups $Y = (B_1 + B_2)$.

Alkoxide formation has been suggested to involve strong basic sites associated with acidic sites of suitable strength (*7*). The models in set C hence define Y as only those $(B_1 + B_2)$ sites which are associated with an optimal acidity. The definition of X_i is that of set B. Comparison of the residuals indicates that the optimal acidity required for alkoxide formation comes from $(A_4 + A_5)$. It is thus suggested that ether formation requires interaction between two types of adsorbed alcohol molecules. One type of alcohol adsorption requires acidic sites associated with weak basic sites i.e., $X_i = (A_i,\ B_4 + B_5)$ and the other chemisorbed alcohol molecules requires an optimal basicity associated with weak acidity i.e., $Y = (B_1 + B_2,\ A_4 + A_5)$. The residual for this model is the least among all models in sets A, B or C.

TABLE 11
GROUP ANALYSIS FIT FOR DIETHYL ETHER FORMATION

Catalyst	Rate[a] ($r \times 10^3$) Predicted	Observed
KSF	2.98	2.98
KSFO	32.04	29.9
KSFO + M	22.30	24.0
F49	13.53	14.20
AHC	1.267	1.20
AHC + M	1.493	1.54
T126	2.267	2.27
F1	0.129	0.129
ALC	2.59	2.39

[a] Specific rates for best model fit are: $f_1 = 914797$; $f_2 = 32852.1$; $f_3 = 6322.86$; $f_4 = 2778.07$; $f_5 = 172.44$.

A comparison of the observed rates with the rates predicted by the group analysis using the best-fit model is shown in Table 11 for diethyl ether and Table 12 for di-

TABLE 12
GROUP ANALYSIS FOR METHANOL DEHYDRATION

Catalyst	Rate[a] ($r \times 10^3$) Predicted	Observed
KSF	3.05	3.05
KSFO	30.53	30.98
KSFO + M	21.6	25.1
F49	13.88	12.47
AHC	2.01	2.00
AHC + M	2.34	2.69
T126	4.54	4.58
F1	0.197	0.197
ALC	3.620	3.25

[a] Specific rates for best model fit are: $f_1 = 937827$; $f_2 = 30046.5$; $f_3 = 9586.5$; $f_4 = 5613.8$; $f_5 = 263.32$.

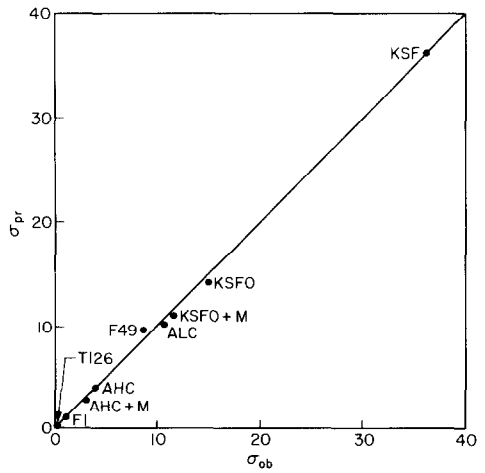

FIG. 5. Group analysis fit for selectivity. Experimental conditions: alcohol concn, 6.64×10^{-3} mol/liter; reaction temp, 200°C.

methyl ether formation. The specific rates reported in Tables 11 and 12 show the effect of acidic strength on f_i. The agreement between the predicted selectivity and the experimentally measured selectivity in ethanol dehydration is shown in Fig. 5.

The details of group analysis showing the actual contributions by each group towards diethyl ether formation are given in Table 13. Comparing the relative contribution of the group with the highest acidic strength in each catalyst, it is apparent with the exception of ALC, all catalysts tested owe above 85% of their ether formation activity to their strongest acidic group. ALC owes its different behavior to a higher number of acidic sites in the A_3 group as compared to the A_2 group as shown in Table 5.

TABLE 13
DETAILS OF GROUP ANALYSIS FOR ETHYL ETHER FORMATION

	Group contribution ($r_{ij} \times 10^3$)				
Catalyst j	$f_1 s_{1j}$	$f_2 s_{2j}$	$f_3 s_{3j}$	$f_4 s_{4j}$	$f_5 s_{5j}$
KSF	2.853	0.115	0.009	0.002	0.002
KSFO	—	30.355	1.217	0.443	0.04
KSFO + M	—	20.70	1.138	0.431	0.055
F49	—	11.393	1.677	0.440	0.040
AHC	—	—	1.092	0.166	0.020
AHC + M	—	—	1.349	0.139	0.013
T126	—	—	—	2.123	0.144
FI	—	—	—	—	0.129
ALC	—	0.745	1.577	0.261	0.024

DISCUSSION

Successful application of group analysis in predicting activity and selectivity of various acid–base catalysts indicates that the relative contributions from various active groups on a catalyst depend exclusively on the number density of sites within each group. The composition or pretreatment history of the catalyst is manifested only through their effect on the site densities in each group. The quantitative correlation of catalyst activities requires a reproducible method of determination of densities and strengths in each effective group of sites.

Although ammonia adsorption capacity and rate recovery experiments exhibit the correct trend of catalytic activities, a quantitative correlation fails partially due to the weaker basicity of ammonia giving the improper resolution but more so because the basicity distributions required for the dehydration activity are not determined by these methods. Calorimetric titrations provide a better method of catalyst characterization yielding both acidity and basicity distributions which can be used for quantitative correlation of relative catalytic activities as indicated by group analysis.

Although the acid–base distributions of various catalysts are characteristics of the surface, they are dependent upon the experimental method (such as calorimetric titrations) employed in their evaluation and they can be used as a unique set of catalyst characteristics only when a standard experimental procedure is adopted. The division of these distributions into groups of different strengths is obviously not unique but is nevertheless suggested by a qualitative agreement with the relative

activities of various catalysts. The value of this division is exhibited in the successful prediction of the rates of both ethylene and ether formation using the same groups for all catalysts. The same groups with similar specific rates yield good predictions of catalytic activities for methanol dehydration.

The models employed to determine s_{ij} in group analysis appear to be in qualitative agreement with the reaction mechanism proposed for the two dehydration reactions, Figueras *et al* (*7*). Ethylene formation requires a dissociative adsorption of ethanol on a strong acidic site associated with a weaker basic site. The strong dependence of the group activity constants on acidity indicate that indeed stronger acidic sites contribute to olefin formation much more effectively than weaker sites. A model based on acidity distribution associated with weak basic sites in the group $(B_4 + B_5)$ results in a better correlative fit than a model based on acidity distribution alone, thus indicating the necessity of weak basic sites for the dissociative chemisorption and subsequent dehydration.

The estimation of the effective site density s_{ij} from the product of site densities in A_i and $(B_4 + B_5)$ inherently assumes a random distribution of acidic and basic sites on the catalyst surface independent of the catalyst composition. Imposition of any particular preference in their relative geometric distributions on the catalyst surface (such as weak acidic sites neighbored by strong basic sites) would lead to different effective site densities s_{ij}. The assumption of randomicity of site distributions leads to successful modeling of catalytic activities, etc., but is by no means proven by such results.

The reaction mechanism for bimolecular dehydration of alcohols leading to ether formation requires an interaction between a dissociatively absorbed alcohol molecule with a surface alkoxide obtained from chemisorption of another alcohol molecule on an acid–base site pair. Earlier mechanistic evidence (*7*) indicates that a strong basic site is effective in alkoxide formation, whereas a strong acidic site is effective in the dissociative adsorption of alcohol and further dehydration. The results of the group analysis using various models to evaluate the effective site density s_{ij} indicate that the best correlative fit is obtained when s_{ij} is evaluated by the product of two separate combinations of acid–base pairs. As in ethylene formation, acidic sites A_i associated with weak basic sites $(B_4 + B_5)$ form one combination, while the other is formed by strong basic sites in the group $(B_1 + B_2)$ associated with weaker acidic sites in the group $(A_4 + A_5)$. The latter combination may be interpreted to represent surface alkoxide formation which requires a strong basic site associated with a weaker acidic site. The exclusion of this combination in evaluating s_{ij} for ethylene formation is in agreement with the reported observation, Knozinger *et al.* (*9*) that the surface alkoxide does not appear in the ir spectra of *t*-butyl alcohol (which forms only olefin upon dehydration) on silica–alumina, and hence is not expected to be an intermediate in olefin formation.

The dependence of s_{ij} for ether formation on basic sites in the groups $(B_1 + B_2)$ associated with acidic sites in $(A_4 + A_5)$ groups appears to explain the alkoxide formation required for the bimolecular dehydration reaction. A better correlative fit using this particular combination of basicity and acidity suggests that although a catalyst surface may exhibit basic sites stronger than $(B_1 + B_2)$, the latter are optimal for alkoxide formation as well as subsequent reaction with the intermediate formed on A_i and $(B_4 + B_5)$ site pair combination. Each acid–base site pair combination included in evaluation of s_{ij} represents different chemisorption steps for the two alcohol molecules and the product of these combinations required for the best correlative fit inherently assumes a random

distribution of these combinations on the catalyst surface as before.

The results of the group analysis show that for most of the catalysts tested, the main contribution to the total activity for both dehydration products comes from a single group involving the strongest acidic sites. The catalyst surface thus assumes a pseudo-homogeneous behavior for these reactions and explains the reason for obtaining the same kinetic model for the catalysts KSFO, F49, AHC and F1 reported earlier (*2*).

CONCLUSIONS

Acid–base distributions obtained by calorimetric titrations provide a useful characterization of acid–base catalysts. These distributions may be divided into groups of sites of different strengths and a group analysis may be applied to correlate the total catalytic activity and selectivity for alcohol dehydration reactions.

The specific rates for both ethylene and ether increase with the acidic strength of the group. The effective site density employed for group analysis assumes random distribution of sites on the catalyst surface and allows for certain acid–base site pair associations consistent with a previously proposed reaction mechanism.

REFERENCES

1. Amenomiya, Y., and Cvetanović, R. J., *in* "Advances in Catalysis" (D. D. Eley, H. Pines and P. B. Weisz, Eds.), Vol. 17, p. 103. Academic Press, 1967.
2. Bakshi, K. R., and Gavalas, G. R., *AIChE J.*, in press.
3. Benesi, H. A., *J. Amer. Chem. Soc.* **78,** 5490 (1956).
4. Bremer, H., and Steinberg, K. H., *Int. Congr. Catal., 4th,* (Moscow), *Prepr.* No. 76 *1968.*
5. Covini, R., Fattore, V., and Giordano, N., *J. Catal.* **9,** 315 (1967).
6. Drushel, H. V., and Sommers, A. L., *Anal. Chem.* **38,** 1723 (1966).
7. Figueras, F., Nohl, A., DeMourges, L., Trambouze, Y., *Trans. Faraday Soc.* **67,** 1155 (1971).
8. Hirschler, A. E., *J. Catal.* **2,** 428 (1963).
9. Knözinger, H., Buhl, H., and Ress, E., *J. Catal.* **12,** 121 (1968).
10. Mone, R., and Moscou, L., *J. Catal.* **30,** 417 (1973).
11. Peri, J. B., *J. Phys. Chem.* **69,** 211 (1965).
12. Pines, H., and Haag, W. O., *J. Amer. Chem. Soc.* **82,** 1471 (1960).
13. Pines, H., and Manassen, J., *in* "Advances in Catalysis" (D. D. Eley, H. Pines and P. B. Weisz, Eds.), Vol. 16, p. 49. Academic Press, New York, 1966.
14. Satterfield, C. N., "Mass Transfer in Heterogeneous Catalysis," p. 33. M.I.T. Press, Cambridge, MA, 1970.
15. Tanabe, K., and Yamaguchi, T., *J. Res. Inst. Catal., Hokkaido Univ.* **11,** 179 (1964).
16. Tanabe, K., "Solid Acids and Bases," Academic Press, New York, 1970.
17. Tarama, K., Teranishi, S., Hattori, K., and Ishibashi, T., *Shokubai* **4,** 69 (1962).
18. Topchieva, K. V., Moskovskaya, I. F., and Dobrokhotova, N. A., *Kine. Catal. (USSR)* **5,** 910 (1964).
19. Walling, C., *J. Amer. Chem. Soc.* **72,** 1164 (1950).
20. Webb, A. N., *Ind. Eng. Chem.* **49,** 261 (1957).
21. Winfield, M. E., *in* "Catalysis" (P. H. Emmett, Ed.), Vol. 7, pp. 93–182. Reinhold, New York, 1960.
22. Yoneda, Y., *J. Catal.* **9,** 51 (1967).